

16 Surface Physics

T. Greber, M. Hengsberger, J. H. Dil (until July 2013), R. Westerström, L. Castiglioni, H. Cun, G. Mette, S. Roth, A. Hemmi, G. Landolt, M. Greif, R. Stania, C. Bernard, L.H. de Lima, A. Schuler, R. Arulanantham, R. Rüttimann, M. Graf, T. Kälin, J. Osterwalder

60

After Hugo Dil, one of our former group members, took up an SNF professorship at EPF Lausanne the group made various adjustments to its research program. Hugo will continue the research on spin-orbit effects at surfaces, including those of topological insulators, performed primarily at the end station *COPHEE* for spin- and angle-resolved photoemission spectroscopy at the Swiss Light Source. This instrument had been built and operated highly successfully by our group over the last decade and a half. Discontinuing this research activity allows the group to strengthen its efforts in the remaining projects and to embark on a new activity on surface-supported catalyst molecules in the context of the University Research Priority Program (URPP) *Light to Chemical Energy Conversion (LightChEC)*. Our continuous efforts for the upscaling of the production of boron nitride and graphene made us a consortium member within the Graphene Flagship of the European Union.

For the investigation of surface and interface phenomena at the atomic level, our laboratory is well equipped for the preparation and characterization of clean single-crystalline surfaces, metal and molecular monolayer films, as well as sp^2 -bonded single layers on surfaces, using a wide variety of experimental techniques. In addition, we take an active role in the commissioning and operation of the new SLS beamline *PEARL (PhotoEmission and Atomic Resolution Laboratory)*. Within the NCCR *Molecular Ultrafast Science and Technology (MUST)*, our group has built and commissioned a compact and mobile angle-resolved photoemission (ARPES) instrument, which is currently taking data at the attosecond laser facility in the laboratory of U. Keller at ETHZ (see Sec. 16.3).

The research carried out during the report period can be grouped into three topics:

- Monolayer films of hexagonal boron nitride (h-BN) and graphene on metal surfaces

Over the past several years the group has gathered considerable expertise in the growth and characterization of sp^2 -bonded monolayers on transition metal surfaces. The strongly corrugated h-BN layer on Rh(111) - termed boron nitride nanomesh - has been further studied with regards to its modification by low-energy ion implantation. Ar^+ ions with en-

ergies of about 100 eV are implanted between the h-BN and the Rh surface layer and immobilized at specific sites of the nanomesh unit cell, forming so-called *nanotents* [1]. The thermal stability of these intercalated species was further characterized [2]. Annealing of these samples leads to the formation of surprisingly regular voids in the film, exposing 2 nm wide patches of metal surface. Implantation of Rb^+ alkali ions was also demonstrated [3].

A second line of research is directed towards the synthesis of epitaxial layers of graphene and h-BN with a view on future electronic devices based on graphene. Due to its insulating properties and similar crystal structure and lattice constant, h-BN appears to be the ideal 'gate oxide'. We have succeeded in growing heterostacks of single-layer graphene on top of single-layer h-BN on Cu(111) and Rh(111) substrates [5, 6]. While the hetero-films are far from defect-free, they allow to study the structural and electronic characteristics of these stacked two-dimensional (2D) materials. Our recent successes in the up-scaling of the growth processes of h-BN monolayers to the wafer scale are described in Sec. 16.1. A considerable effort is currently going on for the development of methods for transferring these layers onto arbitrary substrates.

- Molecular adsorbates and molecular monolayers

One focus here is on single-molecule magnets based on endofullerenes. Recent results on dysprosium-scandium based endofullerenes, measured in the form of thin films far above monolayer thickness, are presented in Sec. 16.2. Experiments with endofullerene monolayers, involving also the interaction of the magnetic moments with the substrate, are currently being prepared at the PEARL beamline.

Within the LightChEC URPP our role is to develop and study model catalyst surfaces that are relevant for solar water splitting. From the group of Roger Alberto from the UZH Chemistry Department we have received a first batch of water reduction catalyst molecules that have shown favourable efficiency and stability in a homogeneous water splitting reactor. A first study of the adsorption behavior of these molecules on Au(111) is ongoing.

- Ultrafast processes at surfaces

After roughly a year of data taking with the MUST photoemission spectrometer attached to the *attoline* at ETHZ [6], a complete set of RABBITT (Reconstruction of Attosecond Beating By Interference of Two-photon Transitions) traces could be fully analyzed and a first paper has been submitted for publication [7] (see also Sec. 16.3). With this method, absolute delays of the photoemission from the valence *d* bands from Ag(111) and Au(111) could be measured. They are on the 100 as scale and vary strongly with energy. These experiments are the first of their kind and give us an unprecedented view on the electron dynamics in solids; they are currently extended to other materials and surfaces.

- [1] H. Y. Cun *et al.*, Nano Letters 13, 2098 (2013).
- [2] H. Y. Cun *et al.*, ACS Nano 8, 1014 (2014).
- [3] L. H. de Lima *et al.*, Rev. Sci. Instrum. 84, 126104 (2013).
- [4] S. Roth *et al.*, Nano Letters 13, 2668 (2013).
- [5] S. Roth, PhD Thesis, Physik-Institut, Universität Zürich, 2013.
- [6] R. Locher *et al.*, Rev. Sci. Instrum. 85, 013113 (2014).
- [7] R. Locher, L. Castiglioni *et al.*, arXiv: 1403.5449 [cond-mat].

In the following, three highlights of last year's research are presented in more detail.

16.1 Boron nitride nanomesh at the 4'' wafer scale

in collaboration with Michael Weinel, Stefan Gsell and Matthias Schreck, Physics Department, University of Augsburg; and the EU FET Flagship Graphene.

A strategic goal of our group has been the production

of 2D materials such as hexagonal boron nitride at large scales. These efforts were well received by the European Flagship Graphene, where our group is part of the ramp-up phase since fall 2013.

We grow single layers of hexagonal boron nitride in a chemical vapor deposition (CVD) process on transition metal surfaces. In the case of a rhodium substrate the so called "nanomesh" structure [1] forms. It was shown that it can not only be produced on expensive single crystals, but also on single-crystalline Rh thin films grown on Si(111) [2, 3]. In 2010 we started with the set-up of a laboratory for the production of single layer materials on the four-inch wafer scale. A new ultra high vacuum (UHV) system is placed in a dedicated clean room environment (ISO class 7). An overview of the laboratory infrastructure is displayed in Figure 16.1. It allows four-inch wafer handling, wafer cleaning, CVD growth of 2D materials and their initial characterization in UHV and in a laminar flow box. Using the single-crystalline metal thin films from the University of Augsburg, this infrastructure is currently used for the growth of boron nitride monolayers [4], but allows more broadly the large-scale fabrication of atomically ordered structures and 2D materials on surfaces.

The need for better control of the growth parameters for the 2D layers led to the development of new in-situ characterization techniques. We succeeded in the construction of an inexpensive growth monitoring system with sub-monolayer sensitivity. It is based on photoemission yield changes that can be measured with an accuracy of 0.4% with a sampling time of one second. The origin of these yield changes are mainly work function changes during growth or modification of an adlayer on the surface [5]. A pulsed ultra-violet light source (Xe flash lamp) induces the photocurrent. Figure 16.2 shows an example

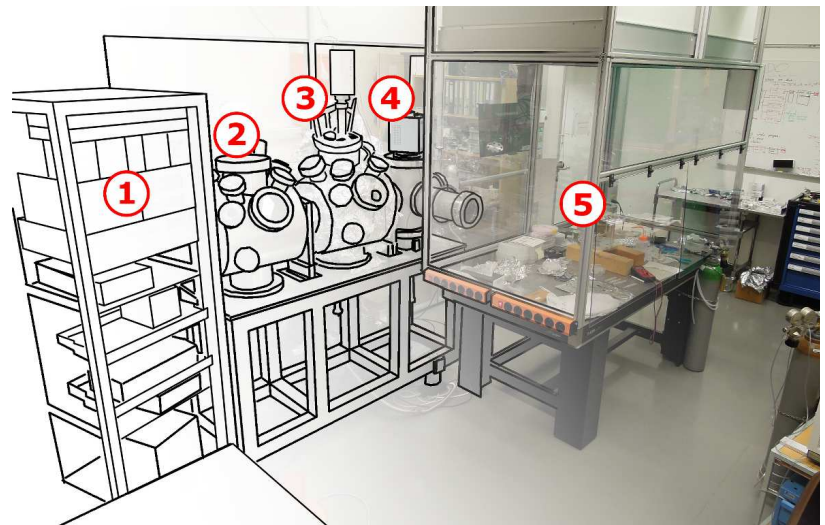
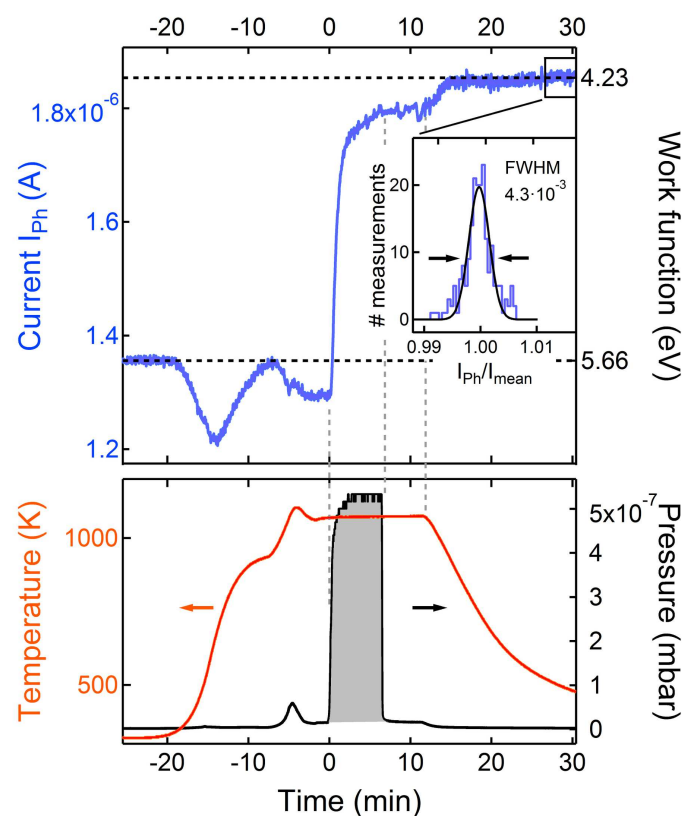


FIG. 16.1 – Schematic view of the laboratory equipment. (1) Electronics rack; (2) analysis chamber; (3) preparation chamber with mass spectrometer; (4) fast entry lock with O₂ plasma cleaner and newly developed four-inch Ar⁺ ion sputtering capability; (5) laminar flow box with access to entry lock and optical table with in air experimental set-up. The complete apparatus is located in a clean room which complies with ISO 7 clean room class requirements.



62

FIG. 16.2 –

The time-evolution of chemical vapor deposition of a hexagonal boron nitride monolayer on a Rh(111) film. Upper part: photocurrent (I_{ph}) as recorded by a collector electrode (solid blue) and the work functions (dashed black) as determined by normal emission UPS measurements before and after this preparation. The inset demonstrates the stability of the current in the indicated box.

Lower part: temperature and pressure observed during the process; the shaded area under the pressure curve corresponds to the dosing of the reaction precursor molecule borazine.

of its capability to observe the growth of a single hexagonal boron nitride layer. The method may be used in pressures up to 1 mbar and is thus perfectly suited for the monitoring of heterostructure growth where significantly higher precursor pressures are required [6].

- [1] M. Corso, *et al.*, *Science* 303, 217 (2004).
- [2] S. Berner, *et al.*, *Angew. Chem. Int. Ed.* 46, 5115 (2007).
- [3] S. Gsell, *et al.*, *J. Cryst. Growth* 311, 3731 (2009).
- [4] A. Hemmi, *et al.*, *Rev. Sci. Instrum.* 85, 035101 (2014).
- [5] A. Hemmi *et al.*, *J. Vac. Sci. Technol. A* 32, 23202 (2014).
- [6] S. Roth *et al.*, *Nano Letters* 13, 2668 (2013).

16.2 Endofullerene nanomagnets

in collaboration with: Alexey Popov, IFW Dresden; Cinthia Piamonteze, Jan Dreiser, and Matthias Muntwiler, Paul Scherrer Institut, Villigen.

The hollow interior of the fullerene carbon cage can be used to encapsulate magnetic clusters that are not found as free species in nature. A fascinating example is the dysprosium-scandium based endofullerenes $Dy_nSc_{3-n}N@C_{80}$ ($n = 1, 2, 3$), where the endohedral unit combines diamagnetic Sc^{3+} and/or paramagnetic Dy^{3+} species at the corners of a triangle with a central N^{3-} ion (Fig. 16.3). Electrostatic interactions with the surrounding ligands, in particular with the central N^{3-} ion, splits the $2J+1$ degenerate ground state into states separated by an energy barrier that prevents a spontaneous reversal of the magnetization. Moreover, the interactions result in a strong axial anisotropy which restricts the individual magnetic moments to orient themselves parallel, or antiparallel, to their magnetic easy axis which is directed along the Dy_n-N bond [1].

At low temperatures, these endofullerenes exhibit a slow relaxation of the magnetization and belong to a class of compounds called single-molecule magnets (SMMs) [2]. They can exhibit magnetic hysteresis similar to traditional macroscopic magnets as well as quantum properties characteristic of a nanoscale entity. Depending on the number of encapsulated Dy ions (n), the endofullerenes exhibit distinct ground state properties like quantum tunneling of magnetization ($n = 1$), remanence ($n = 2$), or frustration ($n = 3$) [1]. The decisive influence of the number of magnetic moments and their interactions is observed in the three significantly different hysteresis curves (Fig. 16.4).

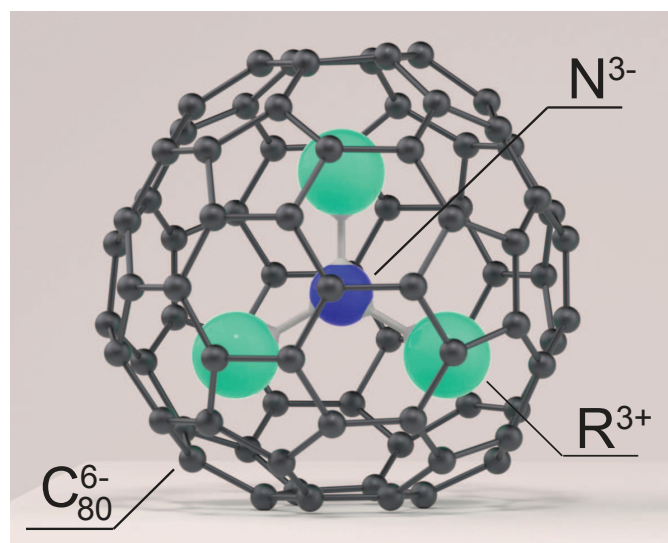


FIG. 16.3 – Model of the nitride cluster fullerene $R_3N@C_{80}$; R = rare earth (here Dy^{3+} or Sc^{3+}).

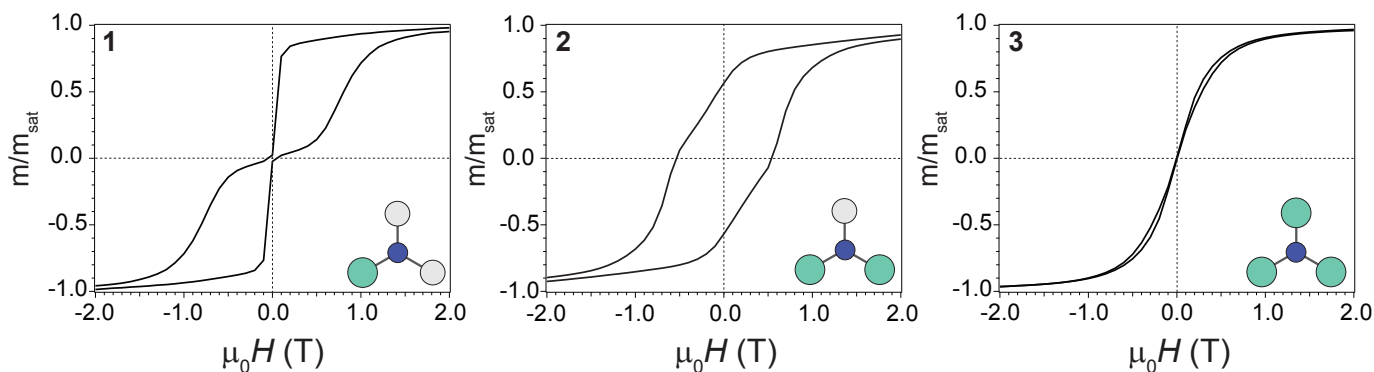


FIG. 16.4 –

Magnetic hysteresis curves recorded from bulk samples of $\text{Dy}_n\text{Sc}_{3-n}\text{N}@C_{80}$ ($n = 1, 2, 3$) using a SQUID magnetometer at 2 K. The cluster compositions are shown as insets with Dy = cyan, N = blue, and Sc = grey. From Ref. [1]

The single-ion dysprosium compound ($n = 1$) was the first endofullerene to exhibit magnetic bi-stability [3]. At low temperatures a butterfly-shaped hysteresis curve is observed with an abrupt drop of the magnetization close to zero-field (Fig. 16.4, left panel). This rapid decay is a consequence of quantum tunneling of the magnetization (QTM) where the magnetic moments are short-cutting the energy barrier separating states of opposite magnetization. When adding a second magnetic moment to the cluster ($n = 2$), the intra-molecular interactions lead to an exchange and dipole barrier which suppresses QTM. This results in a significant remnant magnetization (Fig. 16.4, center panel) with a relaxation time of about 1 h at 2 K. Adding a third magnetic moment to the C_{80} cage produces a ferromagnetically coupled frustrated system, which makes the tri-dysprosium compound ($n = 3$) the softest magnet in the series (Fig. 16.4, right panel).

= 10^{-18} s) timescale due to the characteristic electron velocities and length scales. Recent progress in ultrafast spectroscopy [1] enabled us to study the dynamics of electrons directly in the time domain. Pioneering experiments in gas phase [2, 3] and condensed matter [4] revealed small relative delays between electrons emitted from different initial states.

Reconstruction of attosecond beating by interference of two-photon transitions (RABBITT) [5] was used in gas phase experiments to determine atomic photoemission delays [3]. The extension of RABBITT to noble metal surfaces allowed us to extract energy-dependent photoemission delays from interferometric pump-probe experiments using a short attosecond pulse train in the XUV as pump pulse and a few cycle IR probe pulse [6]. In RABBITT, the absorption of an XUV photon with a specific energy is followed by either absorption or stimulated emission of an IR photon. As shown in Fig. 16.5 this two-photon process gives rise to the appearance of sidebands in the temporal overlap of the XUV and IR pulse. Quantum path interference leads to a beating pattern that entails the spectral photoemission phase.

Our specific experimental setup allows for simultaneous recording of RABBITT traces in a gas and a solid target [7]. The use of photoemission of argon as a temporal reference allowed us to extract absolute photoemission delays from the investigated noble metal surfaces Ag(111) and Au(111) that are depicted in Fig. 16.6 together with the results of our simulations.

The strong variation of the observed delays with energy and in particular the negative delays cannot be reproduced by our simulations that take dipole-transition phase shifts and electron transport to the surface into account. Resonant bulk transitions and many-body effects like screening are likely to contribute significantly to the observed delay times but the theoretical understanding and computation of these effects on attosecond timescales is still in its infancy [8].

- [1] R. Westerström *et al.*, Phys. Rev. B 89, 060406(R) (2014).
- [2] D. Gatteschi, R. Sessoli, *Molecular Nanomagnets*, Oxford University Press, New York, 2006.
- [3] R. Westerström *et al.*, J. Am. Chem. Soc. 134, 9840 (2012).

16.3 Photoemission delays from attosecond interferometry

in collaboration with: Matteo Lucchini, Reto Locher, Lukas Gallmann and Ursula Keller (attoline project), Physics Department, ETH Zurich; NCCR MUST.

Whereas the energetics of the photoelectric effect are well understood and have been studied in great detail, much less is known about its temporal characteristics. Such electronic processes occur on an attosecond (1 as

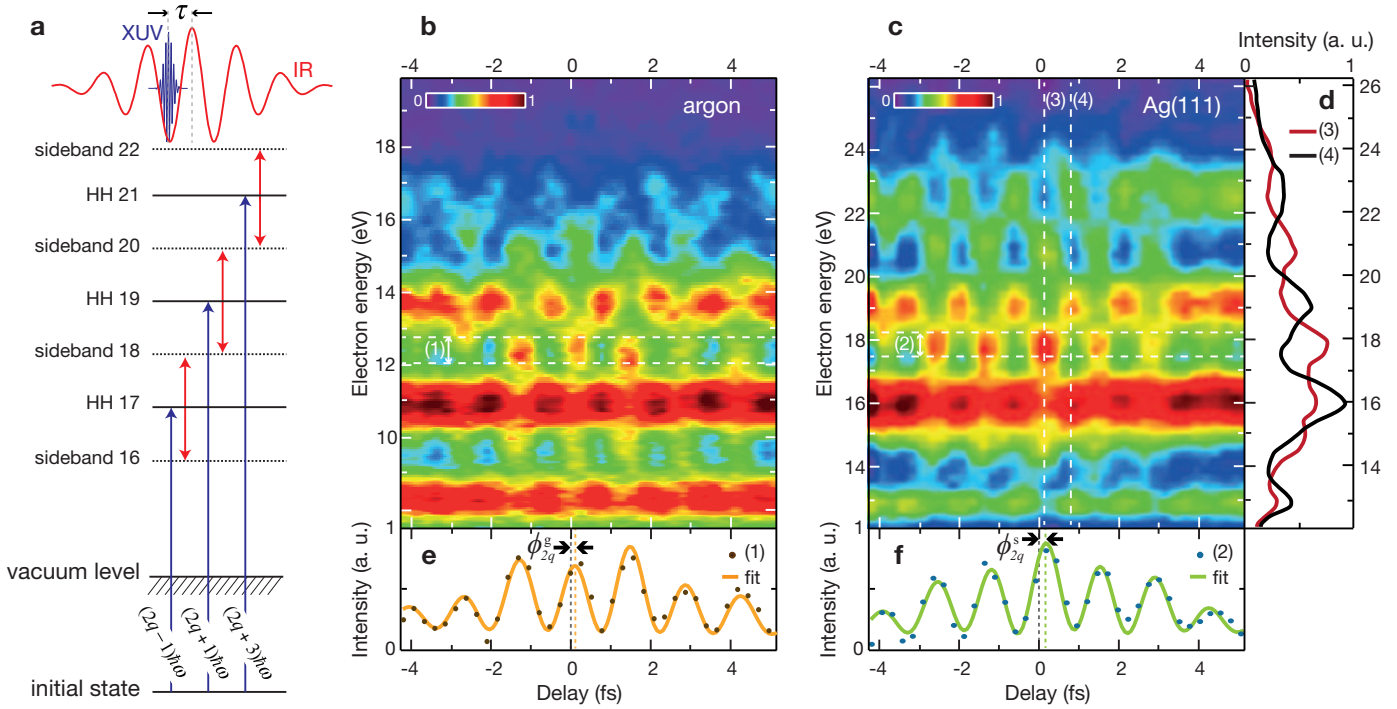


FIG. 16.5 – Experimental RABBITT traces in an Ar gas target and on Ag(111).
 (a) Energy level scheme of the RABBITT process. Interfering two-colour two-photon transitions give rise to sidebands between adjacent odd high harmonics (HH).
 (b, c) RABBITT traces from Ar and Ag(111) with electrons originating from Ar 3*p* and Ag 4*d* levels, respectively.
 (d) Photoelectron spectra from (c) at two different time delays.
 (e, f) Integration over the energy range of sideband 18 revealing the oscillation with 2ω . Experimental curves were fitted with $A(t) \cos(2\omega t - \phi_{2q})$ where ϕ_{2q} is the spectral phase and $A(t)$ is the pulse envelope function.

64

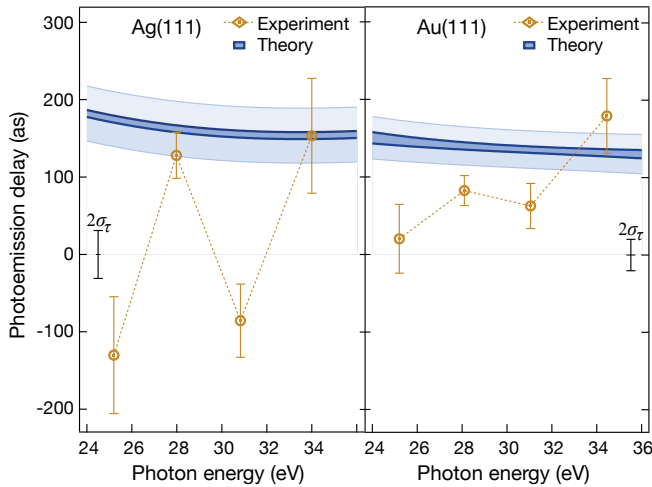


FIG. 16.6 – Photoemission delays for emission from the Ag(111) 4*d*-band and Au(111) 5*d*-band. The measured data are compared with results of our simulations. The $(2\sigma_\tau)$ error bars shown at 0 as indicate the experimental resolution of the propagation delay, τ_{prop} , that results in an uncertainty in the absolute delay scale. The boundaries of the dark blue band indicate the cases with and without screening (upper and lower black lines, respectively). The light-blue shaded band includes σ_τ .

In summary, we built up a new experiment in collaboration with the attoline project at ETHZ, which allows to study light-matter interaction at the fastest possible timescale and sheds new light on the mechanism of the photoelectric effect. Further measurements varying the experimental geometry and electron momenta, as well as investigating more complex samples, are in progress.

- [1] M. Hentschel *et al.*, Nature 414, 509 (2001).
- [2] M. Schultze *et al.*, Science 328, 1658 (2010).
- [3] K. Klünder *et al.*, Phys. Rev. Lett. 106, 143002 (2011).
- [4] A. Cavalieri *et al.*, Nature 449, 1029 (2001).
- [5] P. M. Paul *et al.*, Science 292, 1689 (2001).
- [6] R. Locher, L. Castiglioni *et al.*, submitted for publication (2014); arXiv: 1403.5449 [cond-mat].
- [7] R. Locher *et al.*, Rev. Sci. Instr. 85, 013113 (2014).
- [8] R. D. Muino *et al.*, Proceedings of the National Academy of Sciences 108, 971 (2011).